ELSEVIER

Journal of Nuclear Materials 251 (1997) 1–12

journal of nuclear materials

Defect production due to displacement cascades in metals as revealed by computer simulation

D.J. Bacon *, A.F. Calder, F. Gao

Department of Materials Science and Engineering, The University of Liverpool, Liverpool, L69 3BX, UK

Abstract

Computer simulation using molecular dynamics (MD) can provide information on the mechanisms and final state of defect production in displacement cascades in metals that cannot be obtained by other means. Recent progress in a number of areas in this field is reviewed here. It includes research dealing with the effect on defect formation of primary knock-on atom (PKA) energy, irradiation temperature, the spatial overlap of cascades and alloy additions (solid solutions, ordered alloys and precipitates). It is shown that a rather firm view on dependencies and trends is emerging in all these areas. Improvements still need to be made in some aspects of the simulations for metals, particularly with regard to the accuracy of the interatomic potentials that have to be employed and the neglect of coupling between the ion and electron systems. Nevertheless, the current knowledge of defect numbers, arrangements and properties provided by MD simulation paves the way for future development of models of the evolution of damage beyond the stage of the cascade process. © 1997 Elsevier Science B.V.

1. Introduction

Displacement cascades formed by the recoil of primary knock-on atoms (PKAs) are the principal source of defect production in metals subjected to fast neutron irradiation in power reactor cores. The subsequent evolution of this primary damage can give rise to important changes in the engineering properties of the metallic components and takes place over extended periods of time of the order of years, but models of this long-term behaviour require as their starting point an accurate description of the defect state at the end of the cascade process itself. The processes associated with a displacement cascade occur over length and time scales that are small by the standards of experiment, i.e., nm and ps respectively, and are ideal subjects for study by atomic-scale computer simulation. The aim of the present paper is to demonstrate that computer modelling using molecular dynamics (MD) is a valuable technique for investigating defect production in metals under a range of irradiation conditions.

Atomic-scale computer simulation of displacement cascades over the past decade has confirmed some of the early ideas based on binary-collision concepts and has revealed new aspects not anticipated. This work has been reviewed extensively elsewhere [1–8] and so the present paper will bring some of the issues exposed in the earlier studies up-to-date and emphasise key aspects that have emerged from the modelling. We need to observe at this point that cascades exhibit two main stages as they evolve with time. The first is a ballistic (or collisional) phase lasting a few tenths of a ps for cascade energies of a few keV, during which time the energy of the PKA is distributed by multiple collisions among many atoms, with the result that they leave their lattice sites. This creates a central disordered core surrounded by a mantle of crystalline region displaced outwards. This is shown schematically in Fig. 1. The kinetic and potential components of the crystal energy attain equilibrium with each other during the thermal-spike phase and the majority of the displaced atoms in the outer mantle returns by athermal relaxation to lattice sites in less than one ps. Strong disorder persists in

* Corresponding author. Tel.: +44-151 794 4662; fax: +44-151 794 4675; e-mail: djbacon@liv.ac.uk.

PII S0022-3115(97)00216-X

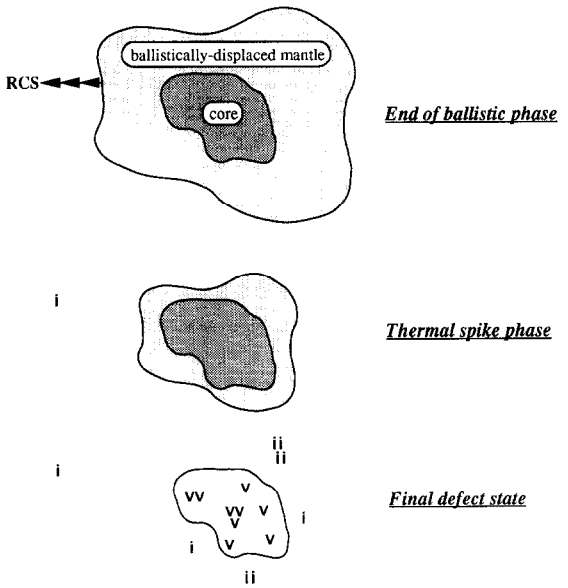

Fig. 1. Schematic illustration of the formation of defects by a displacement cascade. Here, i denotes and interstitial and v indicates a vacancy.

the core for a longer time (several ps), however, and the hot disordered core region has some liquid-like characteristics during the early part of the phase for PKA energies above about 1 keV. The atoms that are unable to regain lattice sites during this final stage form self-interstitial atoms (SIAs) at the periphery of the core and they, and the vacant sites formed when the core crystallises, represent the main cascade contribution to the primary damage state. A few SIAs are created by individual, focused, replacement-collision sequences (RCSs) ejected during the ballistic phase, as illustrated in Fig. 1, but these represent a minor part of the Frenkel pairs produced by cascades.

We shall review results on the effect on defect production of the PKA energy spectrum in Section 2, the intracascade clustering of self-interstitial atoms (SIAs) in different metals in Section 3, the effects of irradiation temperature on defect number and clustering in Section 4, alloy effects in Section 5 and the influence of cascade overlap on defect production in Section 6. Finally, some issues left outstanding, such as the clustering of vacancies and the influence of electron–phonon coupling on defect production, will be discussed in Section 7.

The methods currently employed in cascade simulation by computer will not be dealt with here: they are summarised in [4,7], for instance. We merely note that all the studies referred to have employed many-body interatomic potentials of the embedded-atom or Finnis–Sinclair forms. They were adjusted to describe the atomic interactions at energies that occur throughout the cascade process and are the most realistic that can be used for MD simulations of the scale required for radiation damage.

2. The PKA energy spectrum

The formula due to Norgett, Robinson and Torrens (NRT) [9] has been adopted as the standard for estimating the displacements per atom (DPA) in irradiated metals [10]. It predicts the relationship between the number, N_F, of Frenkel defects, i.e., SIA–vacancy pairs, created by a cascade and the kinetic energy, E_p, of the PKA:

$$N_{NRT} = 0.8\,E_{dam}/2\,\bar{E}_d, \tag{1}$$

where N_{NRT} denotes the value of N_F in the NRT formulation, $\bar{E}_d$ is the value of the threshold displacement energy averaged over all crystallographic directions and E_{dam} is the damage energy available for elastic collisions, i.e., E_p with inelastic losses subtracted. (The NRT formula refers to the damage energy rather than the PKA energy, but since electronic losses are not included in the MD simulations reviewed here, the replacement of E_{dam} by E_p in Eq. (1) is appropriate for comparing N_{NRT} with N_F obtained from simulations.)

The NRT model is based on the binary collision approximation and does not describe how atoms interact in reality during the later stages of the collisional phase and in the thermal spike phase, nor can it predict the spatial arrangement the final defects are likely to adopt. MD simulations do not suffer from these limitations and can be used to study defect production in cascades of relatively large energy and provide direct information on the final number and arrangement of the defects produced. Early simulations of tungsten [11] indicated that N_F is actually a good deal smaller than N_{NRT} for a given cascade energy and this has been confirmed by all the later studies.

The present authors assessed computer-generated defect numbers in [6] to seek an improved relationship between N_F and E_{dam} and an empirical relationship of the form

$$N_F = A(E_p)^m \tag{2}$$

was found to produce an excellent fit to the data for metals of several crystal structures (bcc, fcc, hcp, $L1_2$) and for E_p values up to either 5 keV (Cu, Ti, Zr) or 10 keV (Fe, Ni_3Al). Here, A and m are constants which are weakly-dependent on the material and temperature. The validity of this power-law fit can now be demonstrated more extensively by including more recent data to extend the energy range up to 10 keV for Cu [12] and Ti [14], and 20 keV for Fe [13] and Zr [14]. The complete set of data for an irradiation temperature of 100 K is plotted in Fig. 2. Each data point is the mean N_F value for at least four cascades at that energy. We also include MD data reported in the literature for high energy cascades in Cu [1].

The good fit of the power law (Eq. (2)) to the data reveals its validity, irrespective of the crystal structure. It appears to apply over a wide range of energy. When E_p is expressed in keV, the values for A and m are approximately 5.2 and 0.76, as shown in the table inserted in Fig.

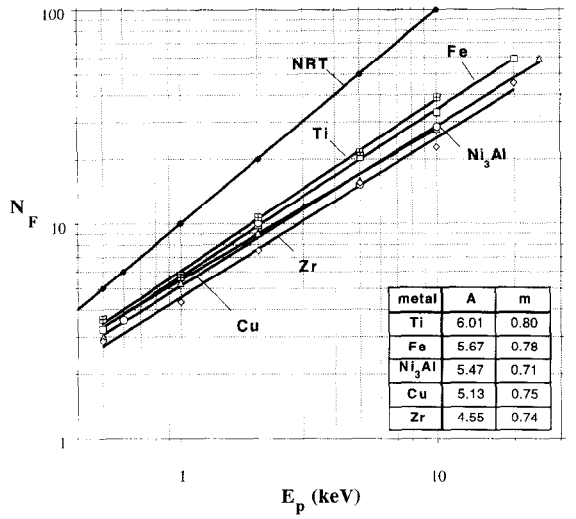

metal	A	m
Ti	6.01	0.80
Fe	5.67	0.78
Ni_3Al	5.47	0.71
Cu	5.13	0.75
Zr	4.55	0.74

Fig. 2. Log–log plot of N_F vs. E_p for four pure metals and Ni_3Al at 100 K, demonstrating the power-law dependence of Eq. (2) in the text. The data are from Refs. [1,6,12–14].

2. As the atomic mass increases, both A and m decrease, suggesting either an enhancement of thermal spike effects or a scaling law arising from an increase in $\bar{E}_d$.

We include in Fig. 2 a line showing the NRT estimate for N_F assuming an $\bar{E}_d$ value of 40 eV. This clearly demonstrates the reduced efficiency with which simulated cascades produce Frenkel defects in comparison with the NRT prediction. This effect is due to the fact that most SIAs are produced not at the end of RCSs but at the periphery of the disordered core (see Fig. 1). The high kinetic energy of the core during the thermal spike assists recombination of SIAs and vacancies. The reduced efficiency compared with the binary collision model was first found experimentally [15] using resistivity measurements to estimate defect production by irradiation at cryogenic temperatures, where defect migration is absent and defect retention therefore a maximum. The MD data are consistent with experiments which imply that defect production efficiency in pure metals and alloys under cascade-producing irradiation with ions and neutrons is approximately one quarter of the NRT value (e.g., [16,17]).

3. Clustering of SIAs

The MD simulations carried out to date predict that a significant fraction of the interstitials created in cascades is produced in clusters, although the size of this fraction depends on the metal [6]. This tendency of defects to cluster in cascades is an important feature in understanding radiation damage (e.g., [18]) because clustering by the end of the cascade process affects defect behaviour and microstructure changes in subsequent evolution of the damage.

Computer visualisations show that some clusters are formed by the end of the thermal spike whereas others arise by short-range diffusion in the first few ps after this stage. Clustering by the latter process occurs as the result of local reorganisation driven by the elastic interaction among neighbouring interstitials and small interstitial clusters. An example of the formation of a 9-interstitial cluster in α-Fe by this means was shown in Figure 17 of Ref. [19]. The vacancies were immobile over the period of the simulation, but the SIAs underwent considerable movement and the final state of the complex was a perfect dislocation loop with a Burgers vector $\mathbf{b} = 1/2\langle 111\rangle$.

Even small clusters of interstitials usually adopt a dislocation-type habit in their stable state. For example, the di- and higher-order-interstitial defects seen in the defect plot in Fig. 3 of the debris produced by a 5 keV cascade in the hcp metal α-Zr can be described as small dislocation loops with $\mathbf{b} = 1/3\langle 11\bar{2}0\rangle$ [20]. (In these plots, each basal-split or basal-crowdion interstitial is revealed as either two atoms sharing one lattice site or three/four atoms sharing two/three sites, respectively. A vacant site is one with no atom situated within 0.3 of the lattice parameter, a_0, of it and vice versa for a displaced interstitial atom.) In dynamic visualisations they are seen to glide back and forth on their glide prism in a one-dimensional migration, as indicated by the arrows on the Figure. Of eight simula-

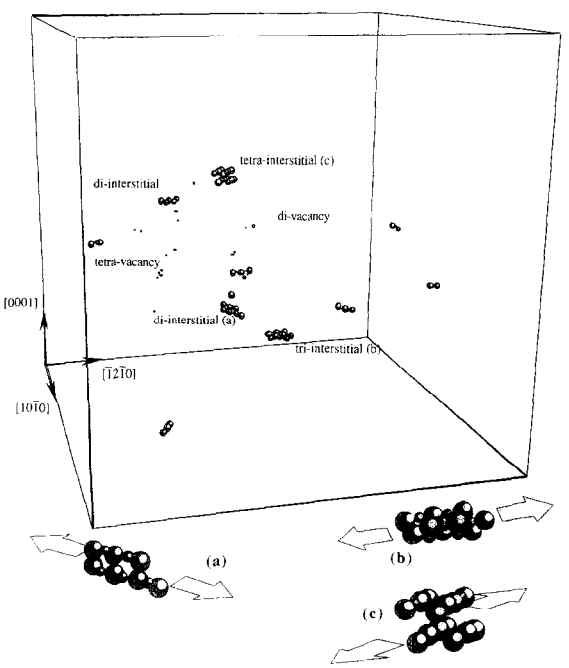

Fig. 3. Final defect state in a 5 keV cascade in α-Zr in a block of 104 832 atoms [20]. The labels indicate the various configurations of vacancies (small spheres) and SIAs (large spheres). The external figures show magnified views of the displaced atoms and vacant sites associated with di-, tri- and tetra interstitials, and their migration directions in the basal plane.

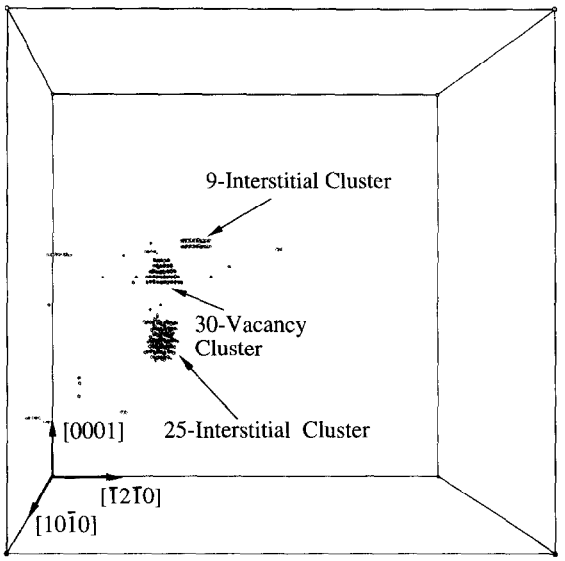

Fig. 4. Final defect state in a 20 keV cascade in α-Zr in a block of 445 536 atoms [14]. The labels indicate the various configurations of vacancies (small spheres) and SIAs (large spheres). The large vacancy and self-interstitial clusters are identified.

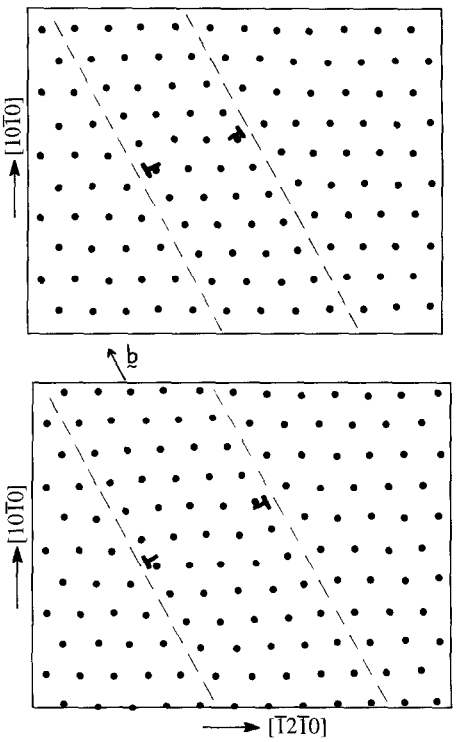

Fig. 5. [0001] projections of the atomic positions in the two basal planes that contain the nine-interstitial cluster shown in Fig. 4. The dashed lines sketched on the figures reveal the glide cylinder and the dislocation symbols indicate the centre of the dislocation core [14].

tions of 20 keV cascades in Zr [14], that with the highest degree of clustering is plotted in its final state on Fig. 4. Here, 9-interstitial and 25-interstitial loops were formed, together with a 30-vacancy loop. The first of these is a glissile, perfect loop, as shown in Fig. 5 by the [0001] projections of the atoms in the two basal planes that contain the 9-interstitial cluster: four SIAs lie in one plane and five in the other. The loop has $\mathbf{b} = 1/3[\bar{1}\bar{1}20]$. The second, larger SIA cluster has a more complex, faulted structure and could not be identified as a simple dislocation.

As implied by comparison of Figs. 3 and 5, the probability of clustering and the size of the largest clusters tend to increase with increasing PKA energy. This is demonstrated by the histogram in Fig. 6 for the cluster statistics for cascades of up to 20 keV in energy in Zr. (For these data, an SIA or a vacancy is a member of a cluster if it has at least one partner in a nearest-neighbour position.) Two striking features of this figure are that a higher proportion of SIAs than vacancies form clusters and that the interstitial clusters created by intracascade mechanisms tend to be as large as the vacancy clusters.

In a comparison [6] of the SIA cluster statistics obtained from the MD simulation of cascades in the five different metals Cu, Fe, Ti, Zr and Ni_3Al, considerable variation was found, with the clustered fraction being highest in copper. To update the data in Ref. [6], we show in Fig. 7 the fraction, f_i^{cl}, of surviving interstitials that exist in clusters of size two or larger in Cu, Fe and Zr at 100 K. It can be seen that the clustered fraction increases strongly at low energy, i.e., in the transition from single displacement events to true cascade phenomena, and above this there is a smaller, but nevertheless significant, variation with PKA energy. The increase with increasing energy

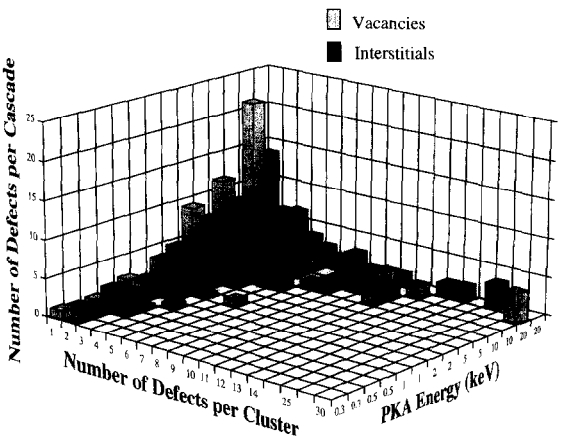

Fig. 6. Data for the number of SIAs in interstitial clusters, and vacancies in vacancy clusters, per cascade as a function of cascade energy in zirconium at 100 K. The data were obtained by averaging over all cascades at each energy [14].

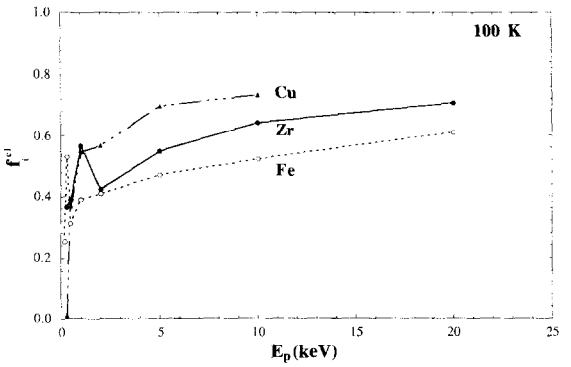

Fig. 7. Variation of the interstitial clustering fraction, f_i^{cl}, as a function of cascade energy for copper, α-iron and α-zirconium at 100 K. The data for Cu and Fe for $E_p = 10$ keV are from Ref. [12], that for Fe at 20 keV is from Ref. [13] and the data for Zr are from Ref. [14].

probably reflects the greater amount of SIA motion that is possible in the longer lifetime of the thermal spike at higher cascade energy.

The clustered fraction is highest in copper and lowest in iron. The difference in behaviour between different metals may be due to the influence of crystal structure on SIA migration. For example, SIAs in the hcp metals become trapped in particular basal planes when they start to cluster (see Figs. 3 and 4 and Refs. [14,20,21]) and, although such clusters are mobile within these planes, their non-basal mobility is low. As another example, the presence of antisite defects may restrict SIA movement in ordered alloys [22]. The ability of SIAs to reorientate and migrate easily during and immediately after the thermal spike may be important for the high level of clustering observed in Cu.

4. The effect of irradiation temperature

In most of the MD simulations of cascades reported in the literature, the PKA was generated in a lattice equilibrated at either 10 or 100 K, which is well below the range of power reactor operation. In a study of the effect of the ambient bulk temperature on cascade damage in both copper and iron, Phythian et al. [12] simulated cascades of up to 10 keV in energy in MD cells equilibrated at either 100 K, 600 K or 900 K. The results for both metals showed a small reduction of the order of 10% in N_F as the temperature is increased from 100 K to 600 K, as first found for iron in Ref. [19], and almost no change on a further increase in temperature to 900 K. However, in these simulations, and those discussed in the preceding sections, the MD cell was treated as an adiabatic system and the redistribution of the PKA energy, E_p, among all the atoms resulted in a rise in temperature of several hundred degrees during the period of the thermal spike. This could affect defect motion and recombination during this phase.

To investigate this further, Gao et al. [23] have recently simulated cascade formation in a crystal at constant ambient temperature. Their method uses the continuum description of heat conduction to calculate the temperature as a function of time in a large block at the ambient temperature, with the continuum parameters calibrated to match those of the atomic system. The temperature distribution of the real MD cell at the end of the ballistic phase of the cascade is imposed as an initial condition, and from this time on, the velocity of atoms in the outer layer of the MD cell is adjusted at each timestep to match the temperature predicted for that region by the continuum model. By making the continuum block much larger than the MD cell and using the initial temperature distribution of the real cascade, the method allows for the variability in shape and energy density between one cascade and another.

This hybrid treatment has been used to study 2 or 5 keV cascades in α-iron at 100 K, 400 K, 600 K and 900 K. The results for N_F are plotted in Fig. 8, where each point is the mean for four cascades for $E_p = 2$ keV and eight cascades for 5 keV, and the bars represent the standard error. The effect on N_F of increasing the irradiation temperature is small but statistically significant: the number of defects produced decreases by about 20–30% as the temperature increases from 100 K to 900 K.

The numbers of Frenkel pairs from the earlier studies [12,19], in which thermal conduction out of the atomic system was not allowed, are shown by the triangular symbols in Fig. 8. The data are in reasonable agreement with those found in the new work, except possibly for the 5 keV cascades at 900 K. This demonstrates that MD simulations without damping at the boundaries are broadly acceptable if the size of the MD model is large enough to avoid overlap of the cascade with itself by virtue of the

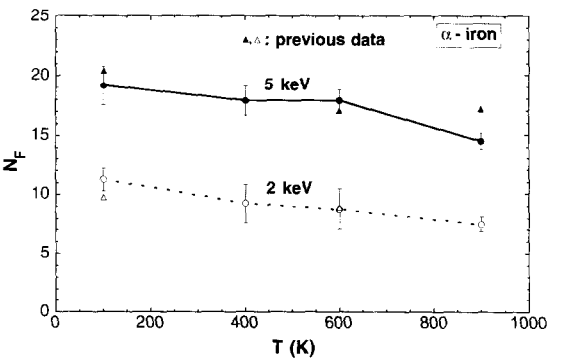

Fig. 8. Data for the number of Frenkel pairs produced per cascade as a function of PKA energy and initial crystal temperature in iron. Data shown as circles were obtained using the boundary treatment developed in Ref. [23]; the triangles are values in Refs. [12,19] where thermal conduction out of the model was not allowed.

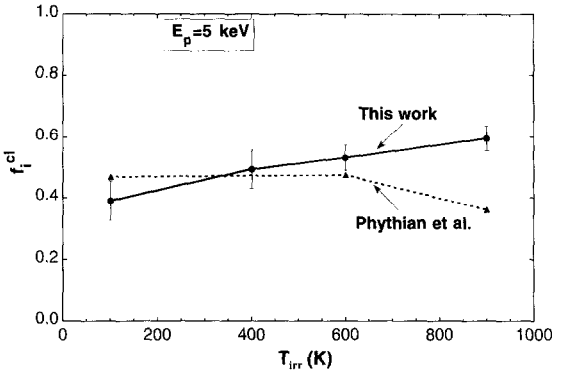

Fig. 9. Variation of the interstitial clustering fraction, f_i^{cl}, as a function of initial lattice temperature for 5 keV cascades in α-iron using data obtained in Ref. [23]. The earlier data from Ref. [12] is shown by the triangular symbols.

periodicity, at least at these energies. The difference in cascade cooling rate due to the more accurate simulation of heat conduction through the lattice ion system seems to have little effect on N_F.

Data for the interstitial clustering fraction, f_i^{cl}, in iron obtained using the new hybrid model are shown as a function of the irradiation temperature for 5 keV cascades in Fig. 9, together with values from the earlier work [12]. The points represent the mean values and the bars the standard error. The new simulations show that an increasing fraction of the decreasing population of interstitials forms clusters as temperature increases over the range considered. The trend is in contrast to the results in [12], where f_i^{cl} in iron and copper had little sensitivity on temperature between 100 and 600 K and then fell significantly by 900 K. We do not know why this difference occurs and cannot explain the earlier results.

5. The effects of alloying on defect production

Although most simulations of cascades in metals have used models of pure elements, several studies have been made of cascades in alloys. Most have been concerned with effects on ordered alloys, where the major effect is the formation of disorder when sites in the lattice become occupied by atoms of the wrong type. MD simulations have shown that this is the dominant product of cascade damage [22,24] and that some alloys become amorphous [25,26], consistent with experiment [27]. We shall not discuss these effects here, but instead will concentrate on simulations which have now been undertaken for cascades in solid solutions and in the vicinity of precipitates.

To study the effect on defect production of alloying elements in solution, Deng and Bacon [28] took copper (atomic mass 63.6 amu) containing up to 15% gold (197 amu) in solution as a model of an alloy with heavy, oversized solute atoms, and simulated cascades of up to 2 keV in energy. In order to investigate the effects of solute mass alone, the same interatomic potentials were also used for an alloy where the solute mass was reduced to only 23 amu.

The simulations for the 'normal' Cu–Au alloy show that the solute influences the ballistic phase by increasing both its duration and the number of atoms displaced temporarily from their sites. The heavy solute atoms restrict the creation of focused collision sequences along individual atomic rows and have a significant effect on the cascade core region. The 'light mass' solutes do not have the same effect. The lifetime and temperature of the thermal spike that follows are strongly enhanced by the gold atoms, as shown in Fig. 10 for the variation with time of the number of atoms with kinetic energy greater than $3k_BT_m/2$ for typical 2 keV cascades, where k_B is Boltzmann's constant and T_m is the melting temperature. Again, the 'light' gold solute does not have the same effect.

This enhancement of the intensity and size of the thermal-spike phase when gold solute atoms are present has two consequences. First, it leads to a large increase in atomic mixing, for the gold solute increases it under all conditions, with a particularly strong effect at the higher concentration [28]. Second, and perhaps surprisingly, the enhanced thermal spike annuls the increase in the number of atoms displaced in the ballistic phase in such a way that the final number, N_F, of Frenkel defects is essentially unchanged by the alloy condition, as shown quantitatively by the mean data values plotted in Fig. 11. It is consistent with simulations of pure metals, which show that cascades that develop a dense form with the largest number of displaced atoms in the ballistic phase tend to end up with the smallest number of Frenkel pairs. This illustrates the importance of the thermal-spike phase in controlling defect production.

Very recently, cascade formation in Fe–Cu alloys has been simulated [29,30]. This alloy system is important

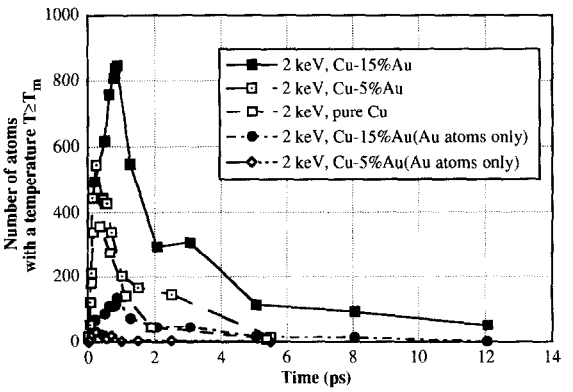

Fig. 10. The number of atoms with kinetic energy greater than $3k_BT_m/2$ as a function of time for a typical cascade with E_p equal to 2 keV [28].

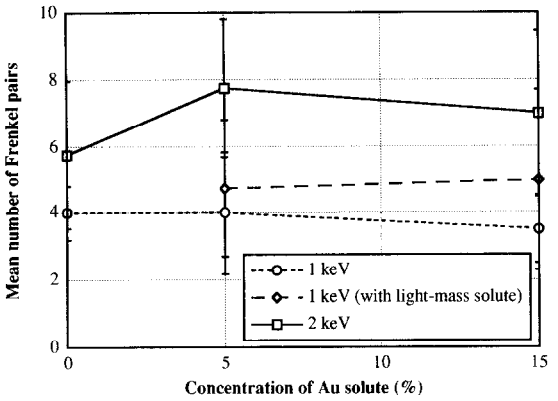

Fig. 11. Variation of the final number of Frenkel pairs with solute concentration [28]. The data are averaged over all cascades at each condition. The bars are the standard error.

because copper in dilute solution in ferritic pressure vessel steels is known to precipitate in the form of small, coherent bcc precipitates during fast neutron irradiation, and these are an important component in the irradiation hardening that occurs during service [31]. The mechanisms that leads to the formation and stability of copper precipitates are not understood, however.

Calder and Bacon [29] have simulated displacement cascades in alloys containing 1% copper in solution using a many-body interatomic potential set. Cascade energy values of 1, 2, 5 and 20 keV energy were considered and six events at each energy were generated in order to provide adequate statistics. The aim was to see if the number of interstitials and vacancies is affected by the presence of copper in solution and if cascades change either the cluster distribution of copper or produce clusters of copper atoms in association with point defects. Care was taken to analyse the distribution of solute before and after a cascade and to compare the distribution of copper atoms neighbouring point defects with that expected statistically.

The number of Frenkel pairs formed by cascades in the alloy was similar to that in pure iron, as may be expected in view of the similar atomic mass and size of copper and iron. Furthermore, no evidence was found for significant Cu–Cu clustering during the cascade process itself, as would have been expected if cascade-assisted nucleation of copper precipitates occurs. The Cu–Cu binding energy is too small and the cascade lifetime too short. The defect statistics did show that a higher than expected fraction of vacancies was produced in first- or second-neighbour sites to copper solute atoms, suggesting that the growth of precipitates during irradiation is controlled by the kinetics of vacancies and copper atoms.

Becquart et al. [30] have reported that in an MD simulation of a 20 keV cascade in a 0.2% solution of copper in iron, a cluster containing iron and copper atoms and vacancies was formed. It is not clear from their report if this defect represents a true clustering of copper atoms by movement from their initial positions or a chance arrangement due to the presence of a vacancy cluster. The interatomic potentials used in [30] produce a larger Cu–Cu binding energy than those in [29] and this may influence the propensity for copper clustering.

The effect of displacement cascades on pre-existing bcc copper precipitates in α-iron was also investigated in [29]. The form of the damage is a function of the relative size of the precipitate and the disordered core zone of the cascade, and the degree of overlap between them. If the precipitate is only partially enveloped by the outer mantle of the cascade (Fig. 1), there is unlikely to be a loss of copper atoms from the precipitate. However, changes to the precipitate are common if it experiences considerable overlap with the core, implying a thermal-spike effect. First, partial dissolution of precipitates by ejection of copper into the iron matrix occurs. The scale of this is not large and no more than two copper atoms were lost from a precipitate in any of the simulations. Second, vacancies were found to accumulate in the copper near the precipitate–matrix interface and interstitials tend to collect near the centre. This effect occurs because vacancies are relatively mobile in precipitates and diffuse to the interface, where a large hydrostatic pressure exists. Interstitials, in contrast, are effectively trapped inside the precipitate by the stress.

6. Cascade overlap effects

Over the lifetime of core components in power reactors, cascades are produced in the debris of earlier cascades, whereas most computer simulation has dealt with single, isolated cascades. At high radiation fluxes, both spatial and temporal overlap may be significant, and even at low dose rates, the consequences of spatial overlap may not be negligible for defect production. We are not aware of any MD studies of temporal overlap, but, as far as spatial overlap is concerned, simulations by Foreman and Phythian [32] have suggested that defect production may be affected when cascades impinge on extended defects such as dislocation loops.

In a more general study, Gao et al. [33] have recently investigated the effect of the spatial overlap of cascades on defect production in α-iron at 100 K. One consideration was the overlap of cascades produced by fast and thermal neutrons. The two cascades have very different energy, for fast neutrons produce cascades initiated by PKAs with an energy typically 5–20 keV, whereas thermal neutrons generate smaller cascades by atoms recoiling with 400 eV from the reaction $^{56}Fe(n, \gamma)^{57}Fe$. The other aspect considered was the overlap of cascades likely to result from a fast flux alone, i.e., PKAs of similar energy in the keV range.

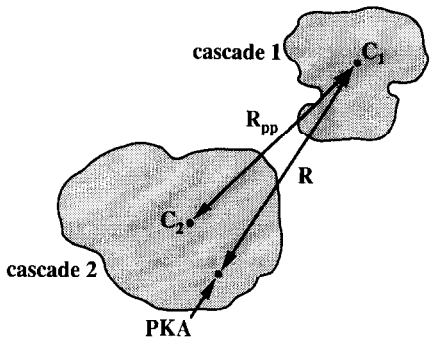

Fig. 12. Schematic illustration of the cascade–cascade separation used in the overlap study [33]. The centre of gravity of the displaced atoms at the peak of the damage of the initial cascade 1 is at point C_1. The second, overlap cascade 2 caused by a PKA at a distance R from C_1 has its damage centred on C_2 at a distance R_{pp} from C_1.

To study these issues systematically, an initial cascade was created with an energy of either 0.4, 2 or 5 keV. The 400 eV and 2 keV debris had N_F values of 4 and 12, respectively. Two states due to initial 5 keV damage were employed, one with $N_F = 24$ and the other 18: the former was used for overlap by 400 eV cascades and the latter for 5 keV events. The second, 'overlap' cascade event was then initiated and the final state of damage assessed. The distance, R_{pp}, between the centres of gravity, C_1 and C_2, of the displaced atoms at the peak in their number at the end of the collisional phase of the two cascades was found to be the pertinent separation distance, as shown schematically in Fig. 12. Values of R_{pp} showed considerable differences from the nominal cascade separation R, and so 104 events were simulated to generate a large data set for the four cascade overlap conditions considered.

Data for the final number of Frenkel pairs as a function of R_{pp} for the four sets of overlap conditions at 100 K are plotted in Fig. 13. The N_F value of the initial cascade is indicated in each case. Despite the statistical scatter, there is a clear trend towards decreasing defect numbers as the overlap distance R_{pp} decreases, indicating a significant defect loss when overlap is strong.

At large R_{pp}, the final number of Frenkel pairs averaged over many simulations is the number from two independent cascades, N_∞, which equals N_F for the initial cascade plus the mean, $\bar{N}_F$, for single cascades of the

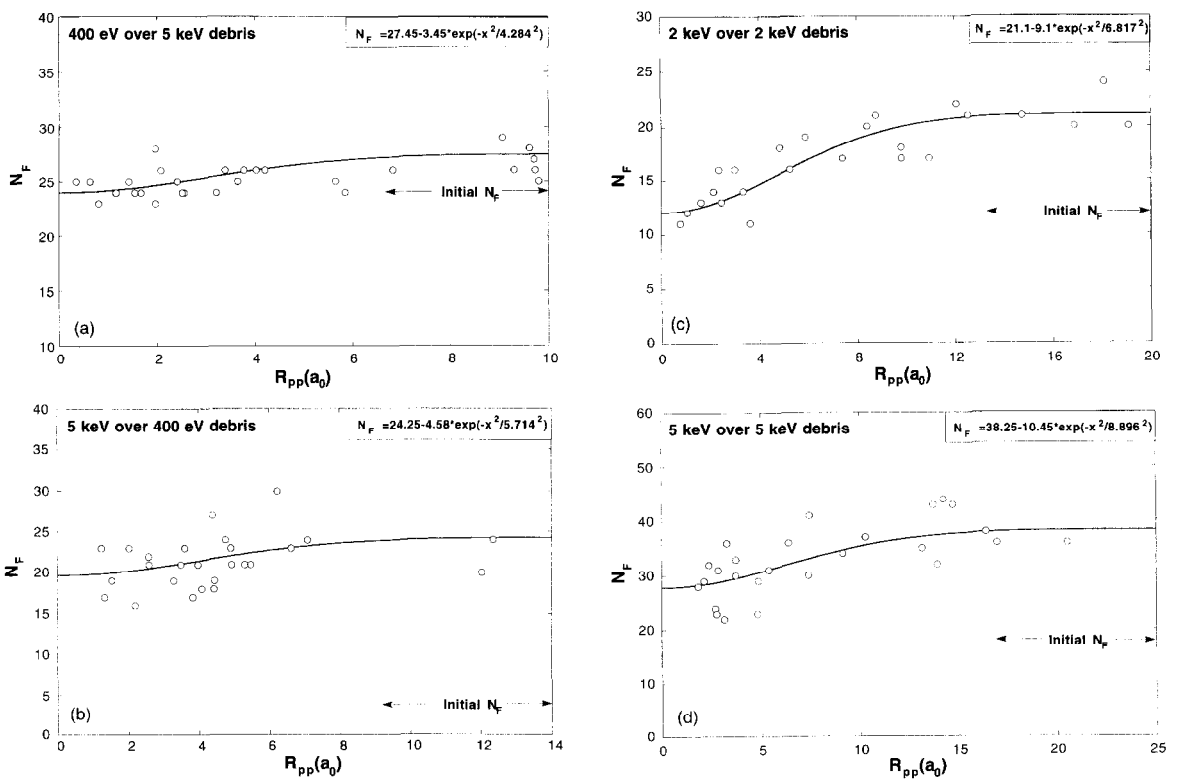

Fig. 13. The total number of Frenkel pairs remaining after the cascade overlap simulations in a crystal at 100 K is plotted as a function of the separation parameter R_{pp} for the four different energy conditions considered [33]. The value of N_F for the initial cascade is given and the best fit of Eq. (3) to the data is shown in the inset.

overlap energy (Eq. (2)). To parameterise the results when overlap is strong, Gao et al. [33] used the mean N_F from data selected for small R_{pp} values at the left of the plots in Fig. 13. Hence, the loss of Frenkel pairs, ΔN, due to overlap is 3.45, 4.58, 9.10 and 10.45 for the four overlap conditions, and compares with $\bar{N}_F$ for single cascades of 3.45, 9.10 and 20.25 for 0.4, 2 and 5 keV, respectively. Several functional fits to the data were considered using only one adjustable parameter. The best was found to be

$$N_F = N_\infty - \Delta N \exp\left(-R_{pp}^2/\Delta R^2\right), \quad (3)$$

where ΔR defines the spatial extent of overlap, i.e., 63% of the defect loss occurs for cascades that overlap within the range $0 \le R_{pp} \le \Delta R$. This function is superimposed on all the data in Fig. 13, and the inset equation reveals the value of ΔR obtained.

For the overlap of a 400 eV cascade with existing 5 keV damage there is a net loss of defects at small R_{pp} that matches the number expected for a single 400 eV cascade. In some cases the strain field of the pre-existing damage seems to defocus and shorten the replacement sequences of the 400 eV event, and thereby promotes recombination, whereas in others the Frenkel pairs of this cascade actually recombine with some of the initial defects. The radius of the sphere that contains 90% of the SIAs produced by a 5 keV cascade is about $6a_0$ on average, so that at small R_{pp} the second cascade may interact with both the vacancies and interstitials of the first or, depending on its shape, occur in a region of crystal containing no defects. The small ΔR value of $4.3a_0$ is consistent with this. The mean loss of Frenkel pairs at complete overlap of the 5 keV cascades with the 400 eV damage is 4.58 and again, therefore, the loss due to overlap is equivalent to the defect production associated with the smaller cascade. However, the mechanisms involved may be different. A 5 keV cascade completely envelops the defects from the 400 eV event when R_{pp} is small and the heat from the thermal spike can induce recombination of prior defects even when they lie outside the hot core. Hence, the overlap parameter ΔR is larger at $5.7a_0$. For the other sets of simulations ΔR increases further due to the increased size of the damage zone. The loss in the 2 keV simulations matches $\bar{N}_F$ for a single 2 keV cascade, but ΔN in the (5 + 5) keV case was about half $\bar{N}_F$ for 5 keV cascades. This is due to the variability of the shape of high energy cascades, for some break up into separate zones and this prevents complete overlap with the pre-existing damage, even though R_{pp} may be small.

Analysis of the number of interstitials found in the overlap simulations shows that while fewer single defects are created in such events, the proportion formed in clusters actually increases above that discussed in Section 3. The mechanisms of this are discussed in Ref. [33].

Gao et al. [33] estimated how important overlap may be in practice, i.e., how significant ΔR is compared with the scale of debris from prior cascades. The broad conclusion was that overlap will become significant for fast neutrons at DPA levels in excess of 1%.

7. Discussion

As noted in Section 1, the many-body interatomic potentials used in the simulations reviewed here are the most realistic available for MD modelling on the scale required for cascade studies, i.e., MD cells containing $\sim 10^4$ to 10^6 atoms. A limitation this imposes is isotropy, i.e., absence of directionality, in the atomic bonds. Unfortunately, more rigorous treatments of metallic bonding, such as ab initio or semi-empirical 'bond-order' methods, cannot be applied to problems on this scale. It is not known to what extent a more accurate description of the interatomic potential for, say, the transition metals would affect the production of defects by the cascade process. Most probably, the ballistic phase and the early part of the thermal-spike phase would not be influenced to a significant extent because many of the atomic interactions occur at short distances where pair terms dominate, but later on angular forces that affect defect behaviour would play a part. This may influence SIA mobility and clustering, for instance, but it seems unlikely that it would seriously alter the general trends for N_F and f_i^{cl} discussed in preceding sections.

It has been demonstrated in Section 2 that the empirical power law (Eq. (2)) relating N_F to the PKA energy E_p provides an excellent fit to the data generated by MD simulations of cascades in metals. The compilation of results suggests that Eq. (2) may have wide applicability, although the physics underlying it has not been explained. Its validity has been shown to apply, irrespective of the crystal structure, over energy levels from a few hundred eV up to several tens of keV. In this context, Stoller et al. [34] have recently found from MD simulations of six 40 keV cascades in iron that N_F equals 132 and therefore falls slightly above the line given by Eq. (2), implying that at high energies where subcascades form, Eq. (2) may no longer be strictly valid because the defect number is then simply the sum of N_F for lower energy events.

Another clear result to have emerged from MD simulations is that SIA clusters form in the cascade process (Section 3). This is consistent with the experimental measurement of diffuse X-ray scattering in copper irradiated with neutrons at 4.6 K [35]. The significance of interstitial clusters for damage accumulation is that these defects are thermally stable and can migrate away from their parent cascades to be absorbed preferentially at sinks such as dislocations and boundaries. Vacancy clusters, in contrast, are not stable and dissociate into individual point defects at high enough temperature. This leads to a 'production bias'

in favour of vacancies in the supply of point defects from cascades [36] and results in the phenomenon of 'void swelling' in some metals. Furthermore, the recombination and clustering that arises within a cascade after the primary damage stage reduce the number of defects that can diffuse three-dimensionally over large distances comparable with the intercascade spacing. (Recent reviews of these topics are to be found in [18,37–40].) It is these 'freely migrating defects' that are responsible for diffusion-driven damage phenomena.

Emphasis in Section 3 was laid on the fact that mobile SIA clusters have a dislocation-like distortion field. Of course, they may not be true Volterra dislocations when only a few interstitials are involved, but an advantage of identifying them as such is that their long-range field can then be approximated rather well by the established results of linear elasticity theory. This is likely to be an important factor for incorporating the description of defect interactions into developments of Monte Carlo models of long-term damage evolution from displacement cascades, such as that presented by Heinisch and Singh [41].

The results from Ref. [23] reviewed in Section 4 are the most comprehensive presented to date on the influence of irradiation temperature on defect production. The data in Fig. 8 show a small, but steady decrease of about 20–30% in N_F as the temperature is increased from 100 K to 900 K in α-iron. By computing the temperature in the cascade core as a function of time, Gao et al. [23] show that the increase in the lifetime of the thermal spike as the ambient temperature increases allows more defect motion to take place before cooling and hence leads to more SIA–vacancy recombination. Data for the interstitial clustering fraction, f_i^{cl}, found in the new simulations (Fig. 9) show that an increasing fraction of the decreasing population of interstitials forms clusters as temperature increases over the range considered. This, again, is due to the more favourable conditions for SIA reorientation and motion that occurs during the longer thermal spike in the metal at higher ambient temperature.

The formation of vacancy dislocation loops, such as are seen experimentally by TEM in heavy-ion-irradiated foils, e.g., [42,43], is a subject of some interest. The fact that loops form at room temperature and below, where vacancies cannot diffuse, reveals the role of the thermal spike. However, the vacancy content of the loops observed can be comparable with the NRT estimate and thus larger than N_F found in computer modelling (Section 2). Furthermore, the actual mechanism that leads to vacancy sweeping and collapse is unclear. Early simulations of 5 keV cascades in copper and nickel [44] suggested that vacancies remain in the liquid-like zone ahead of the resolidification front as it advances during the thermal spike. However, although vacancy clusters are created in most cascade simulations, e.g., Fig. 6, they do not appear to arise, in the main, from a sweeping effect. (The 30-vacancy cluster in Fig. 4 is actually a prism-plane loop and is a possible exception.)

One explanation of this discrepancy between experiment and modelling is that the formation of loops seen in thin foils is assisted by the proximity of a surface. This is indicated by the MD modelling of gold by Ghaly and co-workers [45–48], which suggests that flow of atoms from the molten core of a cascade to a surface can assist vacancy cluster formation. Gao and Bacon [49–51] have confirmed by similar modelling that vacancy loop formation is higher just below a surface in both gold and Ni_3Al, but by a ballistic process rather than the viscous flow envisaged by Ghaly et al. The balance of evidence, however, is that surface-related effects are not responsible for most vacancy loops formed in ion-irradiated foils [50]. It is probable, therefore, that the absence of sizeable collapsed vacancy loops in most simulations of bulk material simply reflects the inadequate conditions that develop in MD models of cascades at the energies considered.

Kapinos and Bacon [52] studied this further by simulating the rapid solidification of a molten zone in a crystal containing vacancies in a one-dimensional heat spike. The vacancy sweeping clearly observed was explained by the need for the liquid to maintain uniform pressure whilst experiencing high temperature gradients. The model has been developed further [53] to treat electron–phonon coupling, which is judged from experiment to be an important material parameter in cascade collapse [54], and it is found that strong coupling can actually prevent both the formation of a true molten zone and its recrystallisation, which are requirements for sweeping and collapse to occur. These ideas have been applied recently in a continuum model to treat the evolution of the temperature and vacancy content of the depleted zone using the thermal and vacancy distributions at the end of the thermal spike predicted by the MARLOWE binary collision code [55,56]. It is assumed that the number and concentration of vacancies have to attain critical values to produce a visible loop by collapse, and that a core with high concentration may not crystallise completely if the rate of cooling is high, such as occurs when the electron–phonon coupling is strong. With physically reasonable values of the critical parameters, the model gives good agreement with the vacancy loop yield and mean loop size found experimentally in ion-irradiated Cu, Ni and Cu–Ni and Cu–Ge alloys.

In this context, the results from Ref. [28] discussed in Section 5 for low energy cascades in copper containing gold in solid solution are of interest because although the presence of the solute leads to a large increase in the number of atoms displaced during the collisional phase, it also produces a strong enhancement in the intensity and lifetime of the spike, with the result that the final number of Frenkel pairs, N_F, is unchanged from that in pure copper. This is in contrast with the ion-irradiation experiments which show that solute concentration as low as 1 at.% can change vacancy retention in loops [57]. Since the enhancement of the thermal spike in the MD simulations only occurred for a very heavy solute at high (= 5 at.%)

concentration, it is a mechanical effect and cannot explain the experimental observations. This, also, supports the interpretation referred to in the preceding paragraph that coupling between the ions and electrons in the hot cascade core may be important for vacancy loop formation. This electronic effect was not included in the MD simulations discussed here.

There is at present no way of allowing for electron–phonon coupling in MD simulation of cascades in an accurate manner. Approximate methods have been developed [58,59], but have not been applied at PKA energies for which vacancy loop formation occurs in experiment. Gao and Bacon [60] have recently used a method similar to that developed by Finnis et al. [58] to investigate the effects of electron–phonon coupling on defect production in cascades of energy up to 10 keV in α-iron. It is found that the final number of defects increases with increasing coupling strength, which is consistent with the fact that, in the approximation used, coupling shortens the lifetime of the thermal spike and reduces SIA–vacancy recombination. Although the size of vacancy clusters increases slightly with the strength, there is no significant change in the number and size of interstitial clusters and the interstitial clustering fraction remains almost constant. At this stage in the modelling of radiation damage, the incorporation of a true picture of electron–phonon coupling, like the more accurate descriptions of atomic interactions, awaits further development.

8. Conclusions

The aim of this paper has been to review recent progress in the MD modelling of defect production in displacement cascades and to highlight issues of interest and concern that have emerged. The important point is that computer simulation can provide information on cascade mechanisms and defect number and configuration that cannot be obtained by other means. There still remain some areas of uncertainty, particularly with regard to the accuracy of the interatomic potentials that have to be employed, the neglect of coupling between the ion and electron systems in metals, and the treatment of technologically-important alloys. Nevertheless, progress has occurred in a number of areas to demonstrate how the primary state of damage production is affected by factors such as PKA energy spectrum, irradiation temperature and cascade overlap, and by material properties such as crystal structure and alloy condition. It has been shown that a rather firm view is emerging on all these matters. This paves the way for future developments in the modelling of damage evolution after the primary defect structure has been created by the cascade process.

Acknowledgements

This research was supported by research grants from the Engineering and Physical Sciences Research Council, Magnox Electric plc and Atomic Energy of Canada Ltd.

References

[1] T. Diaz de la Rubia, M.W. Guinan, Mater. Res. Forum 97–99 (1992) 23.
[2] T. Diaz de la Rubia, W.J. Phythian, J. Nucl. Mater. 191–194 (1992) 108.
[3] T. Diaz de la Rubia, M.W. Guinan, A. Caro, P. Scherrer, Radiat. Eff. Def. Sol. 130&131 (1994) 39.
[4] D.J. Bacon, T. Diaz de la Rubia, J. Nucl. Mater. 216 (1994) 275.
[5] R.S. Averback, J. Nucl. Mater. 216 (1994) 49.
[6] D.J. Bacon, A.F. Calder, F. Gao, V.G. Kapinos, S.J. Wooding, Nucl. Instrum. Meth. B102 (1995) 37.
[7] D.J. Bacon, in: Computer Simulation in Materials Science, eds. H.O. Kirchner, L.P. Kubin and V. Pontikis (Kluwer Academic, Dordrecht, 1996) p. 189.
[8] D.J. Bacon, A.F. Calder, F. Gao, Proc. COSIRES-96, Nucl. Instrum. Meth. B, in press.
[9] M.J. Norgett, M.T. Robinson, I.M. Torrens, Nucl. Eng. Des. 33 (1975) 50.
[10] Standard E521, ASTM Annual Book of Standards, 1989.
[11] M.W. Guinan, J.H. Kinney, J. Nucl. Mater. 103&104 (1981) 1319.
[12] W.J. Phythian, A.J.E. Foreman, R.E. Stoller, D.J. Bacon, A.F. Calder, J. Nucl. Mater. 223 (1995) 245.
[13] R.E. Stoller, in: Microstructure of Irradiated Materials, Symp. Proc., Vol. 373, eds. I.M. Robertson, L.E. Rehn, S.J. Zinkle and W.J. Phythian (Materials Research Society, Pittsburgh, PA, 1995) p. 21.
[14] S.J. Wooding, L.M. Howe, F. Gao, A.F. Calder, D.J. Bacon, submitted to J. Nucl. Mater.
[15] R.S. Averback, R. Benedek, K.L. Merkle, Phys. Rev. B18 (1978) 4156.
[16] P. Jung, J. Nucl. Mater. 117 (1983) 70.
[17] J.H. Kinney, M.W. Guinan, Z.A. Munir, J. Nucl. Mater. 122&123 (1984) 1028.
[18] B.N. Singh, J.H. Evans, J. Nucl. Mater. 226 (1995) 277.
[19] A.F. Calder, D.J. Bacon, J. Nucl. Mater. 207 (1993) 25.
[20] S.J. Wooding, D.J. Bacon, Philos. Mag. A, in press.
[21] S.J. Wooding, D.J. Bacon, W.J. Phythian, Philos. Mag. A72 (1995) 1261.
[22] F. Gao, D.J. Bacon, Philos. Mag. A71 (1995) 43.
[23] F. Gao, D.J. Bacon, P.E.J. Flewitt, T.A. Lewis, J. Nucl. Mater. 249 (1997) 77.
[24] T. Diaz de la Rubia, A. Caro, M. Spaczer, Phys. Rev. B47 (1993) 11483.
[25] M. Spaczer, A. Caro, M. Victoria, T. Diaz de la Rubia, Phys. Rev. B50 (1994) 13204.
[26] H. Zhu, R.S. Averback, M. Nastasi, Philos. Mag. A71 (1995) 735.
[27] D.I. Potter, in: Phase Transformations During Irradiation, ed. F.V. Nolfi (Applied Science, New York, 1983) p. 213.
[28] H.F. Deng, D.J. Bacon, Phys. Rev. B53 (1996) 11376.

[29] A.F. Calder, D.J. Bacon, in: Microstructure Evolution During Irradiation, Sympos. Proc., Vol. 439, eds. T. Diaz de la Rubia, L. Hobbs, I.M. Robertson and G. Was (Materials Research Society, Pittsburgh, PA, 1997) p. 521.
[30] C. Becquart, C. Domain, J. Ruste, Y. Souffez, J.C. Turbatte, J.C. Van Duysen, Proc. COSIRES-96, Nucl. Instrum. Meth. B, in press.
[31] J.T. Buswell, W.J. Phythian, R.J. McElroy, S. Dumbill, P.H.N. Ray, J. Mace, R.N. Sinclair, J. Nucl. Mater. 225 (1995) 196.
[32] A.J.E. Foreman, W.J. Phythian, unpublished work.
[33] F. Gao, D.J. Bacon, A.F. Calder, P.E.J. Flewitt, T.A. Lewis, J. Nucl. Mater. 230 (1996) 47.
[34] R.E. Stoller, G.R. Odette, B.D. Wirth, these Proceedings, p. 49.
[35] R. Rauch, J. Peisl, A. Schmalzbauer, G. Wallner, J. Nucl. Mater. 168 (1989) 101.
[36] C.H. Woo, B.N. Singh, Philos. Mag. A65 (1992) 889.
[37] S.J. Zinkle, B.N. Singh, J. Nucl. Mater. 199 (1993) 173.
[38] L.E. Rehn, J. Nucl. Mater. 174 (1990) 144.
[39] H. Trinkhaus, B.N. Singh, A.J.E. Foreman, J. Nucl. Mater. 199 (1992) 1.
[40] H. Trinkhaus, V. Naundorf, B.N. Singh, C.H. Woo, J. Nucl. Mater. 210 (1994) 244.
[41] H. Heinisch, B.N. Singh, these Proceedings, p. 77.
[42] C.A. English, M.L. Jenkins, Mater. Sci. Forum 15–18 (1987) 1003.
[43] C.A. English, A.J.E. Foreman, W.J. Phythian, D.J. Bacon, M.L. Jenkins, Mater. Sci. Forum 97–99 (1992) 1.
[44] T. Diaz de la Rubia, R.S. Averback, H. Hsieh, R. Benedek, J. Mater. Res. 4 (1989) 579.
[45] M. Ghaly, R.S. Averback, Phys. Rev. Lett. 72 (1994) 364.
[46] R.S. Averback, M. Ghaly, Nucl. Instrum. Meth. B90 (1994) 191.
[47] R.S. Averback, M. Ghaly, J. Appl. Phys. 76 (1994) 3908.
[48] M. Ghaly, R.S. Averback, T. Diaz de la Rubia, Nucl. Instrum. Meth. 102 (1995) 51.
[49] F. Gao, D.J. Bacon, unpublished work.
[50] F. Gao, D.J. Bacon, Philos. Mag. A75 (1997) 1603.
[51] F. Gao, D.J. Bacon, Proc. COSIRES-96, Nucl. Instrum. Meth. B, in press.
[52] V.G. Kapinos, D.J. Bacon, Philos. Mag. A68 (1993) 1165.
[53] V.G. Kapinos, D.J. Bacon, Phys. Rev. B50 (1994) 13194.
[54] D.K. Tappin, I.M. Robertson, M.A. Kirk, Philos. Mag. A70 (1994) 463.
[55] V.G. Kapinos, D.J. Bacon, Phys. Rev. B52 (1995) 4029.
[56] V.G. Kapinos, D.J. Bacon, Phys. Rev. B53 (1996) 8287.
[57] J.S. Vetrano, I.M. Robertson, M.A. Kirk, Philos. Mag. A68 (1993) 381.
[58] M.W. Finnis, P. Agnew, A.J.E. Foreman, Phys. Rev. B44 (1991) 567.
[59] A. Caro, M. Victoria, Phys. Rev. B40 (1989) 2287.
[60] F. Gao, D.J. Bacon, unpublished work.